

and

$$y = \frac{4SG\sqrt{(\pi/P_r)}}{3\rho^*h^*M} \left\{ a_0 \operatorname{erf} \left[\sqrt{\left(\frac{P_r}{2G}\right)} \eta \right] + \Gamma S^{\xi-2n} \frac{a_1}{\sqrt{b_1}} \operatorname{erf} \left[\sqrt{\left(\frac{P_r b_1}{2G}\right)} \eta \right] + \Gamma^2 S^{10-2n} \frac{a_2}{\sqrt{b_2}} \operatorname{erf} \left[\sqrt{\left(\frac{P_r b_2}{2G}\right)} \eta \right] + \dots \right\} \quad (29b)$$

RESULTS AND DISCUSSION

It is clear, from the nature of the radiation function in equation (3) that the effect of radiation is to decrease the enthalpy from its zero-radiation value at any point in the jet. Such decrease will depend on the heat released at the jet entrance and the functional behaviour of the radiation loss on h . Values of h as a function of the distance y from the jet axis are plotted in Fig. 2 by use of equations (20), (24) and (29b) for different values of heat release and for selected values of the other parameters. Shown also in the figure is the zero-radiation solution obtained by both exact and integral methods. It is clear that the integral methods yield a solution which is quite close to that obtained exactly. Therefore, the solution for the enthalpy with radiation obtained by using the integral methods could be considered reasonably accurate.

The decrease in the value of the enthalpy due to radiation will result in an increase in the local density as given by equation (4). Since the momentum at any plane normal to the jet axis is conserved, the increase in the density will result in a decrease in the velocity, except at the jet axis where the velocity is governed by the momentum release at the jet entrance. Representative values of the velocity

distribution versus the coordinate y are shown in Fig. 3. Finally, the dependence of the velocity and the enthalpy distributions on the radiation loss function is shown in Fig. 4 for a fixed value of heat released at the jet entrance. It is clear from the figure that for large values of n , radiation plays an important role on the energy transport in free jets.

REFERENCES

1. S. I. PAI, *Fluid Dynamics of Jets*, Van Nostrand, New York (1954).
2. H. SCHLICHTING, *Boundary Layer Theory*, McGraw-Hill, New York (1955).
3. S. I. PAI, Laminar jet mixing in radiation gasdynamics, *Phys Fluid* **6**, 1440-1445 (1963).
4. M. H. STEIGER and P. K. KHOSLA, On radiating laminar free mixing similarity analysis, Polytechnic Institute of Brooklyn, PIBAL Report No. 810 (1965).
5. M. M. ABU-ROMIA and C. L. TIEN, Appropriate mean absorption coefficients for infrared radiation of gases, *J. Heat Transfer* **89**, 321-327 (1967).
6. C. L. TIEN, Thermal radiation properties of gases, *Advances Heat Transfer*, V, Academic Press, New York (1968).
7. JANAF Thermochemical Tables, PB 168 370, National Bureau of Standards (1965).
8. W. D. HAYES and R. F. PROBSTEN, *Hypersonic Flow Theory*, Academic Press, New York (1959).
9. C. S. YIH, Temperature distribution in a steady laminar, preheated air jet, *J. Appl. Mech.* **17**, 381-382 (1950).
10. M. H. STEIGER and K. CHEN, Further similarity solutions of two-dimensional wakes and jets, *AIAA JI* **3**, 528-530 (1965).
11. M. H. STEIGER and M. H. BLOOM, Further similarity solutions of axisymmetric wakes and jets, *AIAA JI* **3**, 548-550 (1965).

Int. J. Heat Mass Transfer. Vol. 12, pp. 1196-1201. Pergamon Press 1969. Printed in Great Britain

AN EXPERIMENTAL INVESTIGATION OF THE INFLUENCE OF SLOT-LIP-THICKNESS ON THE IMPERVIOUS-WALL EFFECTIVENESS OF THE UNIFORM-DENSITY, TWO-DIMENSIONAL WALL JET

S. C. KACKER and J. H. WHITELAW

Imperial College of Science and Technology, Department of Mechanical Engineering,
Exhibition Road, London S.W.7

(Received 1 January 1969)

NOMENCLATURE

a , constant;
 b , constant;
 m , mass concentration;
 t , thickness of slot lip;

u , velocity in x-direction;
 \bar{u}_c , average velocity through the slot

$$\equiv \frac{1}{y_c} \int_0^{y_c} u \, dy;$$

- u_G , main-stream velocity;
 x , distance along the wind tunnel base-plate, measured from the slot exit;
 y , distance normal to the wind tunnel base-plate;
 y_C , slot height;
 ρ , fluid density;
 ν , kinematic viscosity;
 η , impervious- (or adiabatic-) wall effectiveness

$$\equiv \frac{m_I - m_G}{m_C - m_G}$$

Subscripts

- c , slot;
 G , main-stream;
 I , impervious-wall.

INTRODUCTION

IN AN earlier paper, Nicoll and Whitelaw [1] reported measurements of the impervious-wall effectiveness downstream of a two-dimensional, tangential injection slot. These measurements showed that at downstream distances greater than 25 slot heights, the effectiveness was a maximum when the velocity ratio was approximately unity. A similar trend could be seen in one set of measurements of Seban [2] but, in general, it had not been previously noted. In a subsequent paper [3], the present authors measured the effectiveness with four different values of slot height and demonstrated that, for a given velocity ratio, substantial variations in effectiveness were possible: in the region where the main-stream and secondary mass velocities were equal, the largest slot height gave rise to the highest effectiveness. It appeared from the results described in [3] that the

ratio of slip thickness, t , to slot height, y_C , was the important parameter but, since y_C had been varied, it was possible that changes in mean-velocity profiles had given rise to the changes in effectiveness: the influence of slot-turbulence-intensity was investigated and shown to be small.

The results described in the previous paragraph indicated the need for a detailed series of measurements in which values of effectiveness were recorded as a function of downstream distance, velocity ratio and lip thickness, all other possible parameters being held constant. It is the purpose of the present paper to report the results of an investigation carried out in this manner. A preliminary investigation of this type was reported in Ref. [4] and, although the values of t/y_C were out with the range of those in [3], the trends of both investigations were consistent. As will be shown, the results of the present investigation agree well with those of [3] and [4], and confirm that t/y_C is the important parameter.

APPARATUS AND EXPERIMENTAL PROCEDURE

The experiments were carried out in the wind tunnel, and using the techniques, previously described in [1] and [3]: the general layout is shown in Fig. 1. The slot height was adjusted to 0.247 in. and was constant to within ± 0.002 in. over the centre 12 in. of the wind tunnel. The thickness of the slot lip shown in Fig. 1 was increased by locating additional stainless-steel plates on top of that shown in Fig. 1. These plates had thickness which permitted values of lip thickness of $\frac{3}{32}$, $\frac{5}{32}$, $\frac{7}{32}$, $\frac{9}{32}$ and $\frac{15}{32}$ in. to be attained. They were located with fitted screws.

For experiments with a thin lip ($t = \frac{1}{32}$), the upper-lip-boundary-layer had a virtual origin approximately 7 in. upstream of the slot exit: this was obtained by splitting the flow as shown in Fig. 1. However, for experiments with thicker

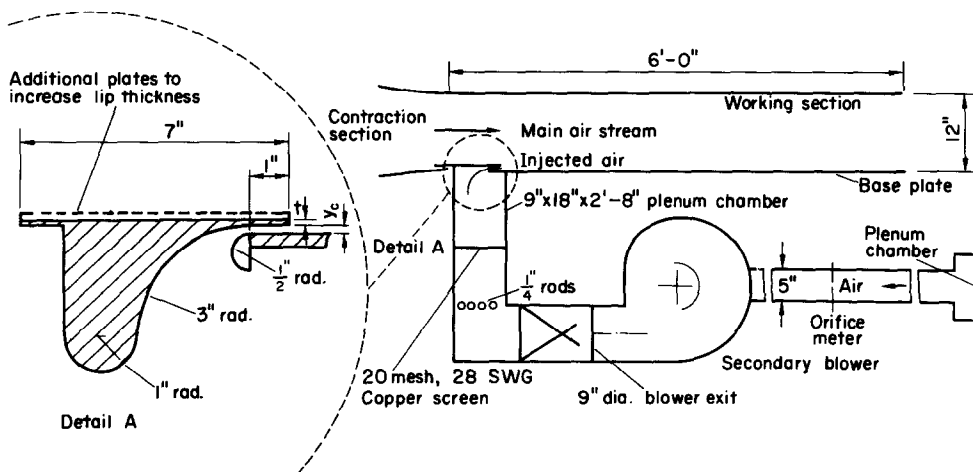


FIG. 1. General arrangement of working section and slot configuration.

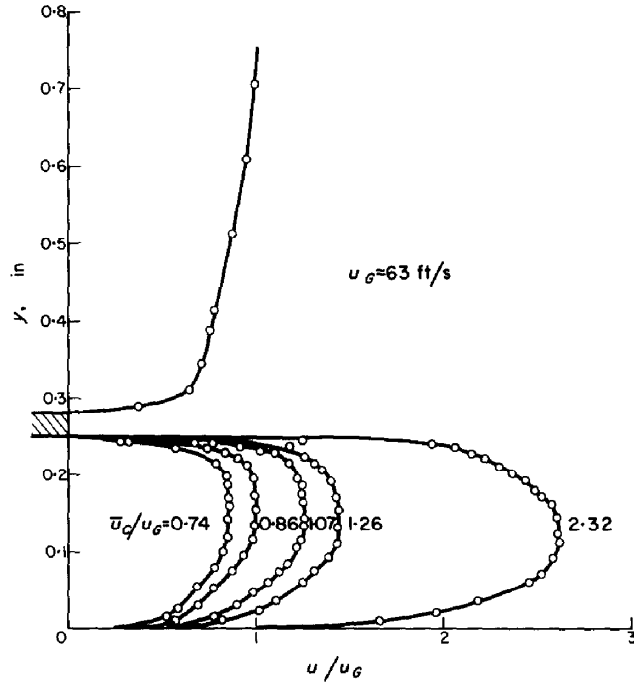


FIG. 2. Measured velocity profiles at the slot exit.

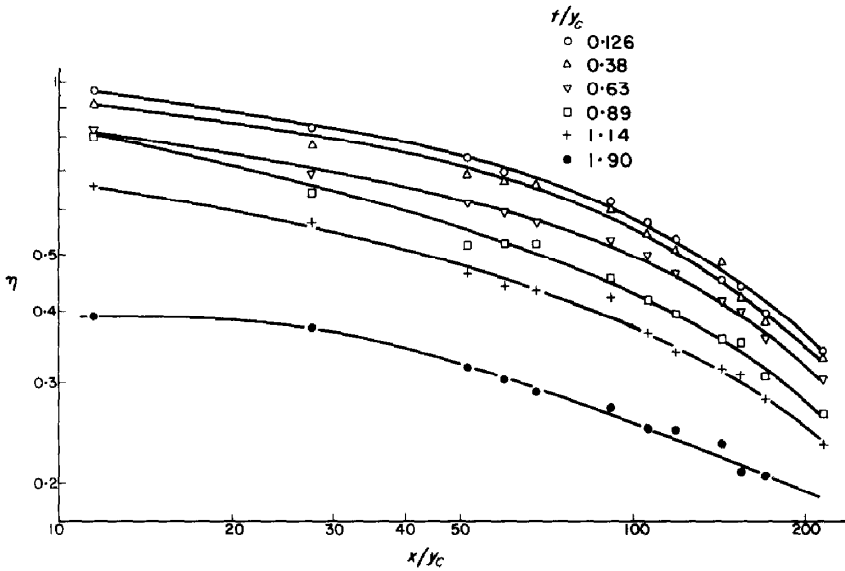


FIG. 3. Impervious-wall effectiveness, $\bar{u}_c/u_0 = 1.07$.

lips, the 'splitting' facility was removed with the aid of sheet metal and tape. The resulting upper-lip-boundary-layer was fully turbulent at the slot exit and had a virtual origin 14 in. from the slot exit. In the present range of velocity ratios, it has previously been shown [5] that very substantial variations in upper-lip-boundary-layer thickness have little effect on the impervious-wall effectiveness.

The effectiveness is shown to depend on the velocity ratio, \bar{u}_c/u_G , and special care was, therefore, taken to ensure that measurements of the impervious-wall effectiveness were obtained for the same values of \bar{u}_c/u_G with each value of t . This could not readily be achieved by integrating mean-velocity profiles measured in the plane of the slot exit since, in thick lip situations, substantial normal pressure gradients were present. Consequently the following sequence was adopted: with the thinnest lip and, therefore, with the smallest normal pressure gradients,† a velocity profile was measured in the plane of the slot exit and integrated to yield

measurements of impervious-wall effectiveness were obtained for the new value of t and the same value of \bar{u}_c . This procedure was repeated for all values of t and thus, since the main-stream velocity was maintained constant at 63 ft/s, values of impervious-wall effectiveness were obtained for sensibly constant values of \bar{u}_c/u_G with each lip thickness. In fact, due to the variation in the static pressure at the slot exit, slight variations in secondary mass flow were noted with the aid of an orifice plate located upstream of the secondary fan; these variations did not exceed $\pm 1\%$ and were considered negligible.

Typical mean-velocity profiles obtained with the thinnest slot-lip are shown in Fig. 2.

RESULTS

Measured values of the impervious-wall effectiveness are shown on Fig. 3 for a value of \bar{u}_c/u_G of 1.07 and for six values of t/y_c : it can readily be seen that the influence of

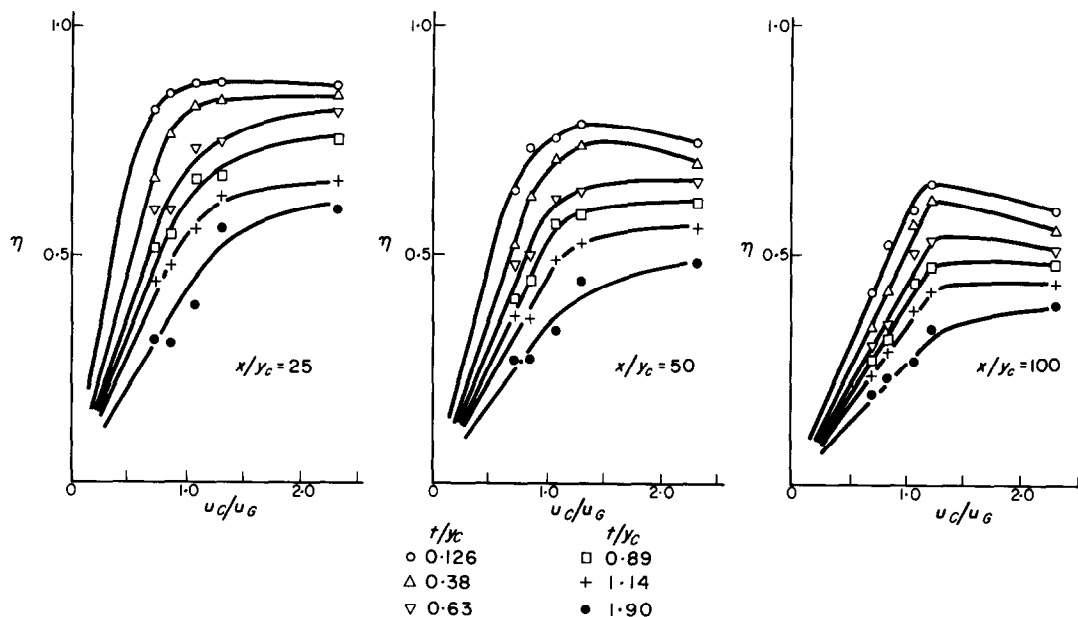


FIG. 4. Impervious wall effectiveness at $x/y_c = 25$, 50 and 100.

a value of \bar{u}_c ; measurements of impervious-wall effectiveness were obtained for this value of t and \bar{u}_c ; without changing the position of the throttle valve on the secondary fan, the slot lip was thickened by the addition of a plate and

t/y_c is substantial. Figure 3 also shows that the maximum deviation of any measured point from the corresponding smooth curve is 0.06 and the mean deviation is considerably smaller. The coordinates of Fig. 3 do not permit all of the present measurements to be conveniently shown, nor do they permit the influence of t/y_c to be clearly shown for values of \bar{u}_c/u_G not close to unity. Consequently Fig. 4 has been prepared. Here the points represent values of impervious-wall effectiveness, interpolated from figures similar to Fig. 3, and corresponding to measured values of \bar{u}_c/u_G and t/y_c .

† Typical static-pressure profiles for a thin lip are presented in [6]; they indicate that the values of \bar{u}_c , for this case, should not be significantly affected by the normal pressure gradient.

DISCUSSION

The results shown in Fig. 4 are in good agreement with those of [3] and [4]: this is demonstrated on Fig. 5. Some differences may be seen at the lower values of t/y_c but the maximum deviation of any measured point from a smooth curve is 0.05. The deviations at the low values of t/y_c are not surprising since, in this region, the influence of small variations in the upstream geometry become important.

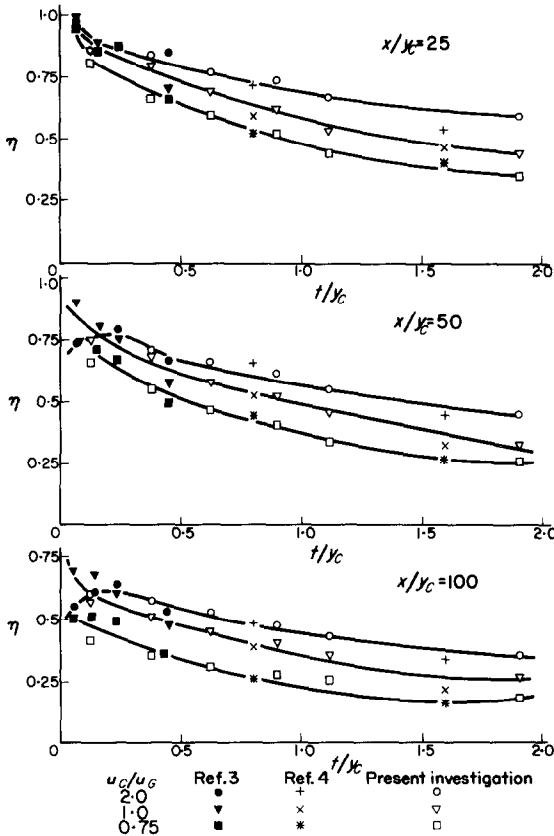


FIG. 5. Comparison of results of refs. [3] and [4] and of the present investigation.

The upstream slot geometry was essentially the same as that used in [3] but the slot has been dismantled and reassembled.

The implications of the results are obvious. The larger the value of the lip thickness, the greater the region of separated flow behind the slot lip, the greater the mixing between the free-stream and the secondary stream and the lower the impervious-wall effectiveness. The effect of lip-thickness is greatest in the region where the velocity ratio is unity. The substantial agreement between the results of the present

investigation, in which y_c was maintained constant, and the results of [3], in which t was maintained constant, confirms that the variations in effectiveness were caused by variations in t/y_c . The possibility that small changes in mean-velocity profiles had caused the variation recorded in [3] can now be discounted. It is the parameter t/y_c which is of greatest importance.

It is likely that the influence of t/y_c can account for discrepancies which exist between the effectiveness measurements of various authors and between their resulting correlations. Certainly, it is clear that the much used correlations of the form

$$\eta \propto \left(\frac{u_G x}{\bar{u}_c y_c} \right)^a \left(\frac{\rho_c \bar{u}_c y_c}{\mu_c} \right)^b$$

are unsuitable for the accurate prediction of effectiveness over a wide range of \bar{u}_c/u_G and t/y_c . Correlations of this form have been used for values of \bar{u}_c/u_G up to 1.5 but the present results show that, in the region close to unity, the influence of t/y_c must be considered. Even for low values of \bar{u}_c/u_G , this form of correlation is unlikely to be satisfactory since a combination of a low value of \bar{u}_c/u_G and a high value of t/y_c leads to the local separation of the secondary flow from the wall. In addition, when t/y_c is very small, the influence of main-stream turbulence intensity and the geometry upstream of the slot exit become important. It is the authors' view that correlation formulae are unlikely to be satisfactory in accounting for all the necessary parameters required for the correct prediction of effectiveness: a more general approach, based upon the solution of the relevant elliptic flow equations is required. The authors are presently directing their attention to an approach of this type.

The present measurements were obtained in constant density flows. It is to be expected that the influence of t/y_c on the impervious-wall effectiveness will diminish as the ratio ρ_c/ρ_G increases and increase as ρ_c/ρ_G decreases. These trends have been confirmed by the measurements of Burns and Stollery [7] and of Pai [8] but a detailed investigation of the influence of t/y_c for various density ratios is still required.

CONCLUSIONS

1. The influence of lip thickness on the impervious-wall effectiveness is confirmed. This influence is greatest in the region of equal main-stream and secondary mass velocities where it is shown that a variation in t/y_c from 0.126 to 1.90 causes a lowering in effectiveness from 0.85 to 0.45 at x/y_c of 25.

2. Attempts to correlate all constant-density, two-dimensional effectiveness data using equations of the form

$$\eta \propto \left(\frac{u_G x}{\bar{u}_c y_c} \right)^a \left(\frac{\rho_c \bar{u}_c y_c}{\mu_c} \right)^b$$

are unlikely to be successful. The parameter t/y_c must be included in the correlation equation.

REFERENCES

1. W. B. NICOLL and J. H. WHITELAW, The effectiveness of the uniform density, two-dimensional wall jet. *Int. J. Heat Mass Transfer* **10**, 623–639 (1967).
2. R. A. SEBAN, Heat transfer and effectiveness for a turbulent boundary layer with tangential fluid injection, *Trans. Am. Soc. Mech. Engrs, J. Heat Transfer (C)* **32**, 303–312 (1960).
3. S. C. KACKER and J. H. WHITELAW, The effect of slot height and slot-turbulence intensity on the effectiveness of the uniform-density, two-dimensional wall jet. *J. Heat Transfer* **90**, 469–475 (1968).
4. S. SIVASEGARAM and J. H. WHITELAW, Film cooling slots; the importance of lip thickness and injection angle, *J. Mech. Engng Sci.* **11**, 22–27 (1969).
5. S. C. KACKER and J. H. WHITELAW, The dependence of the impervious-wall effectiveness of a two-dimensional wall jet on the thickness of the upper-lip boundary-layer. *Int. J. Heat Mass Transfer* **10**, 1623–1624 (1967).
6. S. C. KACKER and J. H. WHITELAW, Some properties of the two-dimensional turbulent wall-jet in a moving stream. *Am. Soc. Mech. Engrs. Paper No. 68-WA/APM-13. J. Appl. Mech.* **35**, 641–651 (1968).
7. W. K. BURNS and J. L. STOLLERY: Film cooling, the influence of foreign gas injection and slot geometry on impervious-wall effectiveness. *Int. J. Heat Mass Transfer* **12**, 938–951 (1969).
8. B. R. PAI, Unpublished measurements.

Int. J. Heat Mass Transfer. Vol. 12, pp. 1201–1206. Pergamon Press 1969. Printed in Great Britain

THERMAL CONDUCTIVITY OF PACKED BEDS AND POWDER BEDS

S. C. CHENG

Mechanical Engineering Department, University of Ottawa, Ottawa 2, Canada

and

R. I. VACHON

Department of Mechanical Engineering, Auburn University, Alabama 36830

(Received 7 October 1968)

NOMENCLATURE

A_{con}	area of continuous phase perpendicular to the xy plane;	p	pressure of two particles against each other;
\bar{a}	accommodation coefficient;	q	integer defined in equation (20);
B	constant in equation (1);	R	thermal resistance;
C	constant in equation (1);	R'	thermal resistance in the microgap;
D	constant in equation (16);	R_L	thermal resistance determined by narrowing of the lines of the heat flow in the region adjacent to the place of contact;
E	Young's modulus;	R_o	thermal resistance of the oxidic film;
H	gas pressure in the pore;	R_{sp}	thermal resistance of microroughness at the place of contact;
H_o	normal gas pressure, ($9.93 \times 10^4 N/m^2$);	r_{sp}	radius of a contact spot;
h	thickness and width of the skeleton of Fig. 1(d);	T	mean absolute temperature of packed beds or powder beds.
h_r	height of particle microroughnesses;		
k	ratio of gas heat capacities at constant pressure and volume;		
k_k	coefficient of particle adhesion;		
k_m, k_n	empirical coefficients, $k_m = (h_r/L) \times 10^3$;		
L	characteristic size of an elementary cell (particle diameter);		
l	characteristic size of a pore;		
n	number of particles in a layer defined in equation (15);		
P_d	discontinuous phase volume fraction;		
Pr_r	Prandtl number;		

Greek letters

ΔR	thermal resistance in a layer;
Δx	small increment in the x axis;
δ	one-half of h ;
η	constant defined in equation (7);
λ_o	gas molecular free path at normal pressure;
λ	thermal conductivity;
λ'	thermal conductivity in the microgap;
λ_o	thermal conductivity of gas at normal pressure;